

Research article

Cadmium immobilization in river sediment using stabilized nanoscale zero-valent iron with enhanced transport by polysaccharide coating

Danlian Huang^{a, b, *}, Zhengxun Hu^{a, b}, Zhiwei Peng^{a, b}, Guangming Zeng^{a, b, **},
Guomin Chen^{a, b}, Chen Zhang^{a, b}, Min Cheng^{a, b}, Jia Wan^{a, b}, Xi Wang^{a, b}, Xiang Qin^{a, b}

^a College of Environmental Science and Engineering, Hunan University, Changsha, Hunan, 410082, China

^b Key Laboratory of Environmental Biology and Pollution Control (Hunan University), Ministry of Education, Changsha, Hunan, 410082, China

ARTICLE INFO

Article history:

Received 20 April 2017

Received in revised form

28 December 2017

Accepted 1 January 2018

Keywords:

Sediment

Nanoscale zero-valent iron

Cadmium immobilization

Leachability

Speciation

Transport

ABSTRACT

Proper management of metal-contaminated sediment plays a key role in sediment recovery and reuse. This study synthesized two kinds of stabilized nanoscale zero-valent iron (nZVI) with starch (S-nZVI) and carboxymethyl cellulose (C-nZVI) for the *in situ* immobilization of Cd(II) in river sediment and investigated their transport in porous media. Experimental data showed that when the sediment sample was treated with C-nZVI for 56 days at a dosage ranging from 5 to 10 mg/g-sediment as Fe⁰, the TCLP (toxicity characteristic leaching procedure) leachability of Cd(II) in the sediment decreased by 93.75–96.43%, and the PBET (physiologically-based extraction test) bioaccessibility of Cd(II) decreased by 22.79–71.32%. Additionally, the acid soluble fraction of Cd(II) was partially transformed to a residual fraction, resulting in a 32.4–33.1% decrease of acid soluble Cd(II) and a 125.4–205.6% increase of the residual-Cd(II) fraction. Surface complexation with iron oxyhydroxide minerals might be the main mechanism of Cd(II) immobilization in sediment. Column experiments indicate that starch or carboxymethyl cellulose (CMC) could extend the travel distance of nZVI, but inherent site physical and chemical heterogeneities still posed challenges for nanoparticle transport. Over all, this study verifies the effectiveness of stabilized nZVI for Cd(II) immobilization in sediment and discusses the potential immobilization mechanism.

© 2018 Elsevier Ltd. All rights reserved.

1. Introduction

River sediment is a basic composition in aquatic ecosystems due to its role as the nutrient source for organisms. Unfortunately, the sediment from rivers or lakes situated near industrial areas, especially mining areas, is being highly polluted with heavy metals (Wang et al., 2014). Cadmium (Cd) is a widespread heavy metal in sediment and is more mobile and soluble than many other metals; thus, this metal can cause direct toxicity for organisms, even at low concentrations (Liu et al., 2009). Like most other metals, the mobility and bioavailability of Cd(II) in soil and sediment are determined by its chemical speciation instead of its total

concentration, and the main objective of many *in situ* remediation technologies is to transform the toxic fraction into an insoluble substance or into a less toxic species (Gil-Díaz et al., 2014a; Huang et al., 2008).

Over the years, iron-based nanoscale particles (such as Fe-Mn, FeS, Fe₃O₄, Fe⁰ nanoparticles) have been widely applied for the removal of heavy metals, including Cd(II), Pb(II), Zn(II), Se(IV) and Cr(VI) from water, due to their strong adsorption or reducing abilities (Arshadi et al., 2014; Boparai et al., 2013; Huang et al., 2015; Ling et al., 2015; Xu et al., 2012). Subsequently, the immobilization of heavy metals in soil and groundwater using iron-based nanoscale particles has also recently attracted attention (Cheng et al., 2016; Gil-Díaz et al., 2014a; Su et al., 2016; Xie et al., 2015). However, the use of nanoscale zero-valent iron (nZVI) for the *in situ* immobilization of Cd(II) in soil or sediment has been rare. On the other hand, the transport behaviour of nZVI is directly related to whether nZVI can reach the contaminated subsurface zones and capture the target contaminants, so an investigation of the transport of nZVI in sediment is also needed. Due to the nanosize particles and large specific surface areas of nZVI, it is probable that

* Corresponding author. College of Environmental Science and Engineering, Hunan University, Changsha, Hunan, 410082, China. Tel.: +86 731 88822754; fax: +86 731 88823987.

** Corresponding author. College of Environmental Science and Engineering, Hunan University, Changsha, Hunan, 410082, China. Tel./fax: +86 731 88823701.

E-mail addresses: huangdanlian@hnu.edu.cn (D. Huang), zgming@hnu.edu.cn (G. Zeng).

nZVI aggregates easily, making nZVI undeliverable to the contaminated subsurface zones and, thus, unusable for *in situ* applications. To avoid rapid agglomeration, our group has developed various stabilizing strategies by using sodium alginate and sodium dodecyl sulfate as stabilizers (Huang et al., 2015, 2016). In addition, types of conventional polysaccharide stabilizer, starch (He and Zhao, 2005) and CMC (Ambika et al., 2016) are also popular due to their well stabilized performance, nontoxicity and biodegradation. Hydroxylated macromolecules in starch and CMC, which contain size-confined nanoscale pools of inter- and intramolecular origins, can promote the nucleation and crystallization of nZVI (He and Zhao, 2005). In addition, the molecules act as multidentate ligands, forming strong coordination bonds with nZVI to overcome the van der Waals or magnetic forces of attraction between nZVI (Ambika et al., 2016). Therefore, the use of starch or CMC could change the size and dispersibility of nZVI and significantly improve its transport in porous media (He and Zhao, 2007).

As reported by previous researcher (Boparai et al., 2013; Zhang et al., 2014), nZVI can not reduce the heavy metal ions (Cd^{2+}) to zero valent metals (Cd^0) because the standard potentials of cadmium and zero-valent iron are nearly identical:



While Calderon et al. reported that nZVI could form the iron oxyhydroxide minerals (amorphous Fe(II)/(III) (hydr)oxide, i.e., α -, β -, γ -FeOOH) layer during nanoparticle synthesis and ageing (Calderon and Fullana, 2015). In addition, the relative stability of Cd(II) adsorption complexes on the FeOOH has been confirmed by Randall et al. (1999). Thus, adsorption or surface complex formation on the formed iron oxyhydroxide layer may be the most likely mechanism of Cd(II) immobilization.

In the present study, the effectiveness of starch- and CMC-stabilized nZVI for Cd(II) immobilization in sediment and nanoparticle transport in porous media were investigated. The main objectives were (a) to prepare and characterize the desired stabilized nZVI using water-soluble starch or CMC as a stabilizer; (b) to investigate the effects of the stabilizers, particle dosage and treatment time on the TCLP (toxicity characteristic leaching procedure) leachability/PBET (physiologically-based extraction test) bio-accessibility of Cd(II) and Cd(II) speciation; (c) to examine the nanoparticle transport in ideal and heterogeneous media; and (d) to analyse the potential mechanism of Cd(II) immobilization using stabilized nZVI. The research might be particularly significant to engineers, practitioners and sediment-repair company managers because these results could lead decision-makers to use nanotechnologies, which are novel in environmental management, into practice. Additionally, the application of nZVI in metal-contaminated sediment provides a new direction for sediment recovery and reuse.

2. Materials and methods

2.1. Materials

All the chemicals were analytical grade or higher. Water-soluble

starch and CMC were purchased from the Tianjin Damao Chemical Agent Factory (Tianjin, China). Other chemicals were obtained from Sinopharm Chemical Reagent Co., Ltd. All solutions and suspensions were prepared with ultrapure deionized (DI) water (18.25 Ω , Milli-Q Millipore).

River sediment samples from the shallowest 25 cm were collected from the Xiang River in Hunan, China. Before use, the sediment samples were air-dried for one month and passed through a 2-mm sieve. The key sediment physicochemical characteristics are included in Table 1. The Cd(II) concentration in the sediment (22.50 mg/kg) was more than 18 times that of the sediment quality guidelines for metals (Cd(II): 1.2 mg/kg) (Burton, 2002). According to the potential ecological risk index (RI) (Hakanson, 1980), the potential risk of Cd(II) was 2045, which was much higher than those of Pb (48) or Cr (7) (Table S1). According to the European Community Bureau of Reference (BCR) sequential extraction procedure (Wan et al., 2016), the mobility and bioavailability of the three metals were calculated and compared, and they followed the sequence of Cd > Pb > Cr (Fig. S1).

2.2. Synthesis and characterization of stabilized nZVI

Stabilized nZVI was synthesized using the modified method described by He et al. (He and Zhao, 2005). Before use, DI water and stabilizer solution were purged with purified N_2 for 30 min to remove the dissolved oxygen. The preparation was carried out in a 250 mL three-necked round bottom flask attached to a nitrogen line. Traditionally, a 25 mL $\text{FeSO}_4 \cdot 7\text{H}_2\text{O}$ stock solution was added to a 100 mL stabilizer solution and was left to stir for 30 min to form starch- or CMC- Fe^{2+} . Then, the Fe^{2+} ions were reduced to Fe^0 by adding stoichiometric amounts of sodium borohydride solution dropwise into the mixture. When all of the sodium borohydride solution was added, the mixture was stirred for another 30 min. The whole period was kept at inert conditions to ensure the efficient use of the reducing agent BH_4^- . The concentrations of the $\text{FeSO}_4 \cdot 7\text{H}_2\text{O}$ solution used in this study were 14.9 and 29.8 g/L. Accordingly, the stabilizer concentrations were either ~0.2% (w/w) for 0.5 g/L Fe^0 or ~0.4% (w/w) for a 1.0 g/L Fe^0 suspension. Bare-nZVI (B-nZVI) was also prepared via a similar method but in the absence of starch or CMC. Three kinds of nZVI suspensions were used for batch and column experiments after their synthesis.

Newly synthesized nanoparticles were dried in a vacuum drying oven (DZF-6020, Shanghai) at 80 °C for 8 h and were then ground into a fine powder in a nitrogen atmosphere. The nanoparticles were stored in brown bottles filled with nitrogen gas before their characterization. The hydrodynamic diameters of the nanoparticles were determined via dynamic light scattering (DLS) using NaNoZS (Malvern, UK). Scanning electron microscope (SEM) images of nZVI were taken by a JSM-6700F (JEOL, Japan). Fourier transform infrared spectrometry (FTIR) (Nicolet, USA) was performed at a spectral range varying from 4000 to 400 cm^{-1} . The x-ray diffraction (XRD) patterns of the nanoparticles were observed using a Philips-X'Pert Pro MPD (Netherlands) with a high-power Cu-K α radioactive source ($\lambda = 0.154 \text{ nm}$) at 40 kV/40 mA.

2.3. Sediment treatment with stabilized nZVI

The sediment samples were amended by mixing 0.5 g of stored

Table 1
Physicochemical characteristics of the river sediment used in this study.

Parameter	pH	CEC (cmol/kg)	TOC (%)	OM (%)	Cd (mg/kg)	Cr (mg/kg)	Pb (mg/kg)	Sand (%)	Silt (%)	Clay (%)
Sediment	7.6	21.6	3.49	6.02	22.50	159.80	221.77	65	32	3

sediment (dry weight) with 5 mL of nanoparticle suspension (0.5 or 1.0 g/L) or DI water in 15 mL (50 mL) plastic centrifuging tubes, resulting in a suspension-to-sediment ratio of 10:1 (mL/g). The mixtures were sealed and shaken for several minutes and were then held still at room temperature (25 ± 1 °C) for the desired days. For typographical convenience, the treatment at a Fe^0 concentration of 0.5 g/L is denoted as case 1 (5 mg/g-sediment as Fe^0), and that at 1.0 g/L is denoted as case 2 (10 mg/g-sediment as Fe^0). Reaction times varied from 0 to 56 days. The mixture was centrifuged at 3000 rpm after each treatment, and the supernatant was collected and analysed for the subsequent Cd(II) mass balance calculations. The treated sediment samples were used for further TCLP, PBET and BCR tests. To ensure data quality, all sediment treatment tests were performed in triplicate.

2.4. TCLP tests

TCLP tests are acknowledged as the standard method to determine the leaching toxicity of Cd(II) in sediment (Jiang et al., 2004). This method was listed in S4 in the Supplemental Data.

2.5. PBET tests

An in vitro test system called PBET was conducted to predict the Cd(II) bioavailability in DI water and nanoparticle treated sediment (Ruby et al., 1996). The method was listed in S5 in the Supplemental Data.

2.6. BCR sequential extraction of sediment-bound Cd(II)

BCR sequential extraction procedure was applied to determine the influence of the tested nanoparticles on the changes in the Cd(II) speciation. The method was listed in Table S2. The precision of the data was evaluated via their recovery rates by dividing the sum of the four fractions by the total Cd(II) content. The recovery rates of Cd(II) in this experiment ranged from 94% to 107%, which agrees well with other studies (Wan et al., 2016; Wen et al., 2016).

2.7. Column experiment

Column experiments were conducted using glass columns (CT Chromatography Equip Co., Ltd, Jiangyin) with 1.6 cm internal diameter packed with either quartz sand or sediment-supplemented quartz sand for a packed bed height of 12 cm. Half of the sediment-supplemented quartz sand was sediment and the other was quartz sand. The size distribution of the quartz sand and sediment sample are shown in Fig. S2. Prior to packing the glass columns, the quartz sand and sediment-supplemented quartz sand were pretreated using the method described in the literature (Basnet et al., 2015; Jaisi and Elimelech, 2009; Pelley and Tufenkji, 2008; Quevedo and Tufenkji, 2012). Quartz sand and sediment-supplemented quartz sand column experiments were conducted as described by Pelley (Pelley and Tufenkji, 2008) and Basnet (Basnet et al., 2015), respectively. Prior to injecting nanoparticles, the breakthrough behaviour of an inert tracer (10 mM KNO_3) was monitored to evaluate the packed bed performance, and then 6 pore volumes (PV) of the nanoparticle suspension were filtered. $\text{NO}_3\text{-N}$ was indirectly determined via ultraviolet spectrophotometry (Wu et al., 2017). The iron concentration was indirectly measured using a Hach DR 2800 Portable Spectrophotometer (Kambhu et al., 2012). The columns were placed vertically to simulate natural groundwater conditions.

2.8. Data analysis

The data sets were analysed using the one-way ANOVA procedure of SPSS v19.0 (IBM, USA). The differences between the means were determined using Duncan tests and were assigned a significance threshold of $P < .05$.

3. Results and discussion

3.1. Characterization of stabilized nZVI particles

Fig. 1A shows the chain-like aggregates of spherical B-nZVI. In contrast, the stabilized nZVI is discrete and has a more uniform shape than that of B-nZVI. In addition, both stabilized nZVI have obvious membranes on the surface of nZVI, indicated with the red arrows in Fig. 1B and C. Based on DLS analysis, the mean hydrodynamic diameters of S-nZVI and C-nZVI were 277.3 ± 11 nm and 209.3 ± 9 nm respectively, while the mean hydrodynamic diameter of B-nZVI was greater than 1000 nm, possibly because the B-nZVI could aggregate rapidly in water (Chen et al., 2012).

Compared with the FTIR spectra of B-nZVI [Fig. 1D (a)], changes in the peaks of S-nZVI [Fig. 1D (b)] and C-nZVI [Fig. 1D (c)] were observed. Peaks at 3313 cm^{-1} and 3349 cm^{-1} , corresponding to the O-H stretching bond from starch or CMC, were detected but were not detected in B-nZVI. This result indicates that starch and CMC had attached to the nZVI surfaces (Lin et al., 2010). Additionally, shifts from 3382 cm^{-1} to 3313 cm^{-1} and 3349 cm^{-1} suggest an enhancement of the strength of the intermolecular hydrogen bonds between the stabilizers and nZVI (Ambika et al., 2016; He et al., 2007). In Fig. 1D, we found that the apparent peaks at $\sim 2100\text{ cm}^{-1}$ disappeared in the C-nZVI and S-nZVI samples [Fig. 1D (b) and (c)]. It is possibly because the peaks near $\sim 2100\text{ cm}^{-1}$ represent the C=O stretching vibration in starch and CMC (Maity and Agrawal, 2007; Lian et al., 2013), while the C=O bond might be unstable in the synthesis of stabilized nZVI. Fig. 1D also revealed a shift from 1662 cm^{-1} to 1606 cm^{-1} for S-nZVI and from 1616 cm^{-1} to 1604 cm^{-1} for C-nZVI. An and Zhao (2012) reported similar shifts and attributed them to the decrease in the strength of the covalent bonds resulting from the inhibition of the conjugation of COO^- when attached to the nZVI surface. However, the peak appearing at 1683 cm^{-1} for B-nZVI might be due to the C-O from CO_2 in air (Maity and Agrawal, 2007). Furthermore, new peaks with low wavenumbers ($<700\text{ cm}^{-1}$) corresponding to the Fe-O stretches of iron oxides confirm the partial oxidation on the surface of nZVI, which was not clearly obvious for C-nZVI [Fig. 1D (c)], suggesting that CMC showed a better stabilization effect.

The XRD patterns of B-nZVI, S-nZVI and C-nZVI are shown in Fig. 1E, which highlights the formation of iron oxides in the synthesis of nZVI. A diffraction peak of $2\theta = 44.8^\circ$ indicated the crystallization of Fe^0 (Weng et al., 2013). Furthermore, the XRD patterns of B-nZVI indicate the presence of maghemite ($\gamma\text{-Fe}_2\text{O}_3$, $2\theta = 39.5^\circ/55.68^\circ$), magnetite (Fe_3O_4 , $2\theta = 36.5^\circ$) and lepidocrocite ($\gamma\text{-FeOOH}$, $2\theta = 66.28^\circ$) [Fig. 1E (a)], which were not detected in S-nZVI and C-nZVI (Huang et al., 2016; Kim et al., 2013; Lin et al., 2010; Shi et al., 2011). This result was consistent with the result obtained from FTIR and can be explained by the stabilizing effect of starch and CMC.

3.2. Effects of nanoparticle treatment on Cd(II) immobilization in sediment

3.2.1. TCLP leachability of Cd(II)

The TCLP leachability of Cd(II) in the control at various treatment times was detected to be $\sim 0.224\text{ mg/L}$, which was lower than the concentration stipulated by the EPA regulation (1 mg/L) but still has potential toxicity for organisms (Moral et al., 2002). In Fig. 2, we

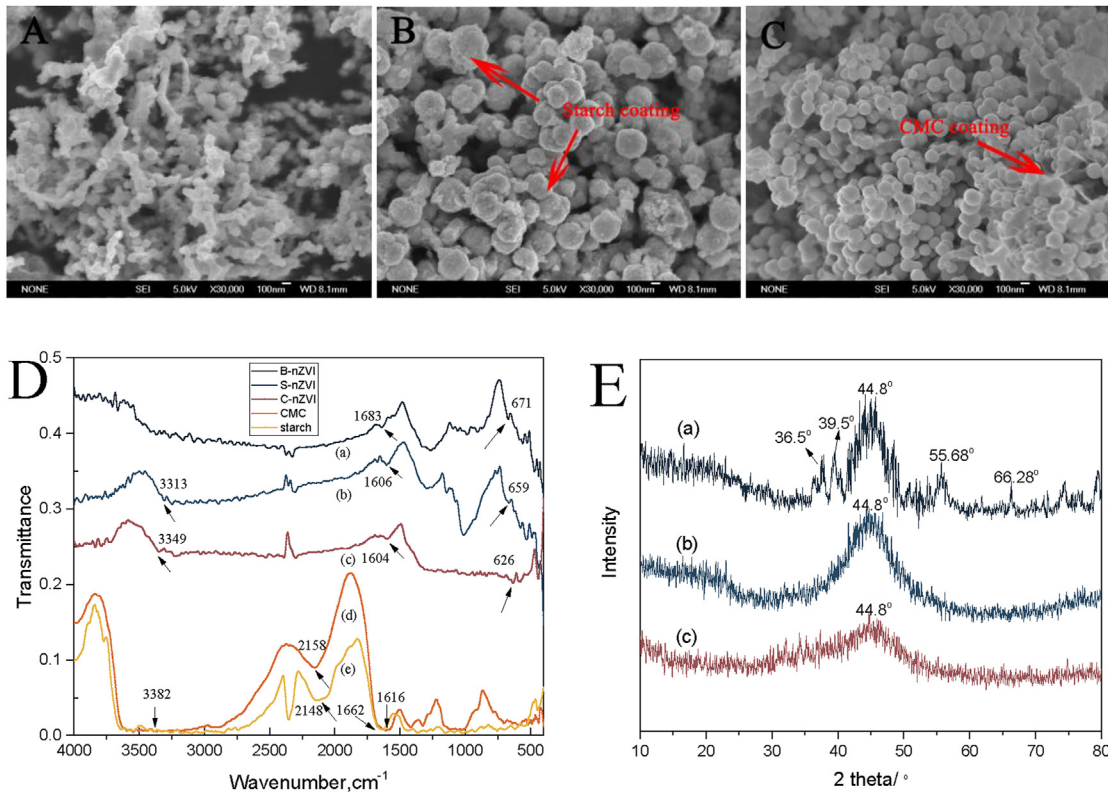


Fig. 1. Characterization of synthesized nZVI. SEM images of the nZVI prepared at 0.5 g/L as Fe^0 with: (A) no stabilizer (B-nZVI), (B) 0.20 wt% starch (S-nZVI), and (C) 0.20 wt% CMC (C-nZVI). (D) FTIR spectra of samples: (a) B-nZVI; (b) S-nZVI; (c) C-nZVI; (d) CMC; (e) starch, arrows indicate the peaks of corresponding functional groups. (E) XRD pattern of samples: (a) B-nZVI; (b) S-nZVI; (c) C-nZVI.

found that when the sediment samples were treated with nanoparticle suspensions for 14 days, as in case 1 (Fig. 2a), the Cd(II) leachability decreased from its original 0.219 mg/L to 0.113 mg/L, 0.126 mg/L and 0.082 mg/L, i.e., 48.40%, 42.47% and 62.56% immobilization efficiencies (Eq. S(6)), respectively ($P < .05$) (Fig. 2b). The Cd(II) leachability was further reduced with the reaction time in both cases, especially in case 2, wherein it was sharply lowered to 0.010 mg/L, 0.009 mg/L and 0.008 mg/L after 56 days of treatment by B-nZVI, S-nZVI and C-nZVI, respectively ($P < .05$) (Fig. 2c). Compared with case 1, case 2 exhibited an enhanced effect on the reduction of the TCLP-leachable Cd(II). This result can be attributed to the greater adsorption sites provided by the Fe^0 in case 2 (Randall et al., 1999). Additionally, following 14 days of treatment by B-nZVI, S-nZVI and C-nZVI, significant decreases in Cd(II) leachability levels were found in both cases, suggesting that 14 days is a critical period for Cd(II) immobilization. However, the Cd(II) leachability from the 14th to 56th days was reduced by only ~1%, resulting in a ~96% overall immobilization efficiency in case 2, which differs markedly from that in case 1. From the scope of the nanoparticle mass transfer and the reaction kinetics, the observations show that the Cd(II) immobilization is kinetically the most effective within 14 days, and equilibrium is nearly reached at 14 days, as shown in case 2 (Liu and Zhao, 2007). It was also found that S-nZVI and C-nZVI generally performed better than B-nZVI. This phenomenon could be explained by the nanosize effect of stabilized nZVI, such that the smaller size might react more easily with Cd(II) (Wan et al., 2016). In summary, the results above suggest that the stabilized nZVI is an effective *in situ* amendment for the TCLP leachability of Cd(II) in Cd-contaminated sediment.

3.2.2. PBET bioaccessibility of Cd(II)

The *in vitro* bioaccessibility of Cd(II) was measured using the PBET method, in which a much higher solution-to-solid ratio (100:1) and a much harsher solution of pH 2.3 were applied to mimic the GI tract (Chou et al., 2009; Gebelein et al., 2003; Lee et al., 2011; Sharp and Turner, 2013). Fig. 3 shows the PBET bioaccessibility of Cd(II) and its immobilization efficiency (Eq. S(7)) in sediment. In the control groups, the Cd(II) bioaccessibility was up to ~0.140 mg/L (~62.5% of the total Cd(II) content) in various treatment time, which was markedly higher than the TCLP leachability (~20%). A similar observation was found for nanoparticle treated sediment samples (Fig. 3a and c). This result agrees well with that of Chou et al. (2009), who evaluated the biotoxicity of PBET and TCLP leachate from fly ash and bottom ash, and attributed the much more PBET-based bioaccessibility of Cd(II) to the low pH in the PBET extraction solution. In fact, the Cd(II) in the Xiang River sediment is mainly presented in the form of acid dissolvable ion and iron/manganese oxides-bound form (Huang et al., 2016; Wen et al., 2016), and the latter could resist leaching in moderately acidic solutions, such as the TCLP liquid due to the buffering capacity of the sediment (Liu and Zhao, 2007). However, under PBET conditions, the sediment buffering capacity was exhausted, and the bound-Cd(II) was mostly released.

3.2.3. Speciation of Cd(II)

According to the BCR sequential extraction procedure, heavy metal Cd(II) in the sediment can be divided into four speciations: acid soluble (AS), reducible (RE), oxidizable (OX) and residual (RS). The mobility and bioavailability of Cd(II) follow the sequence of $\text{AS} > \text{RE} > \text{OX} > \text{RS}$ (Wang et al., 2015). In the original sediment,

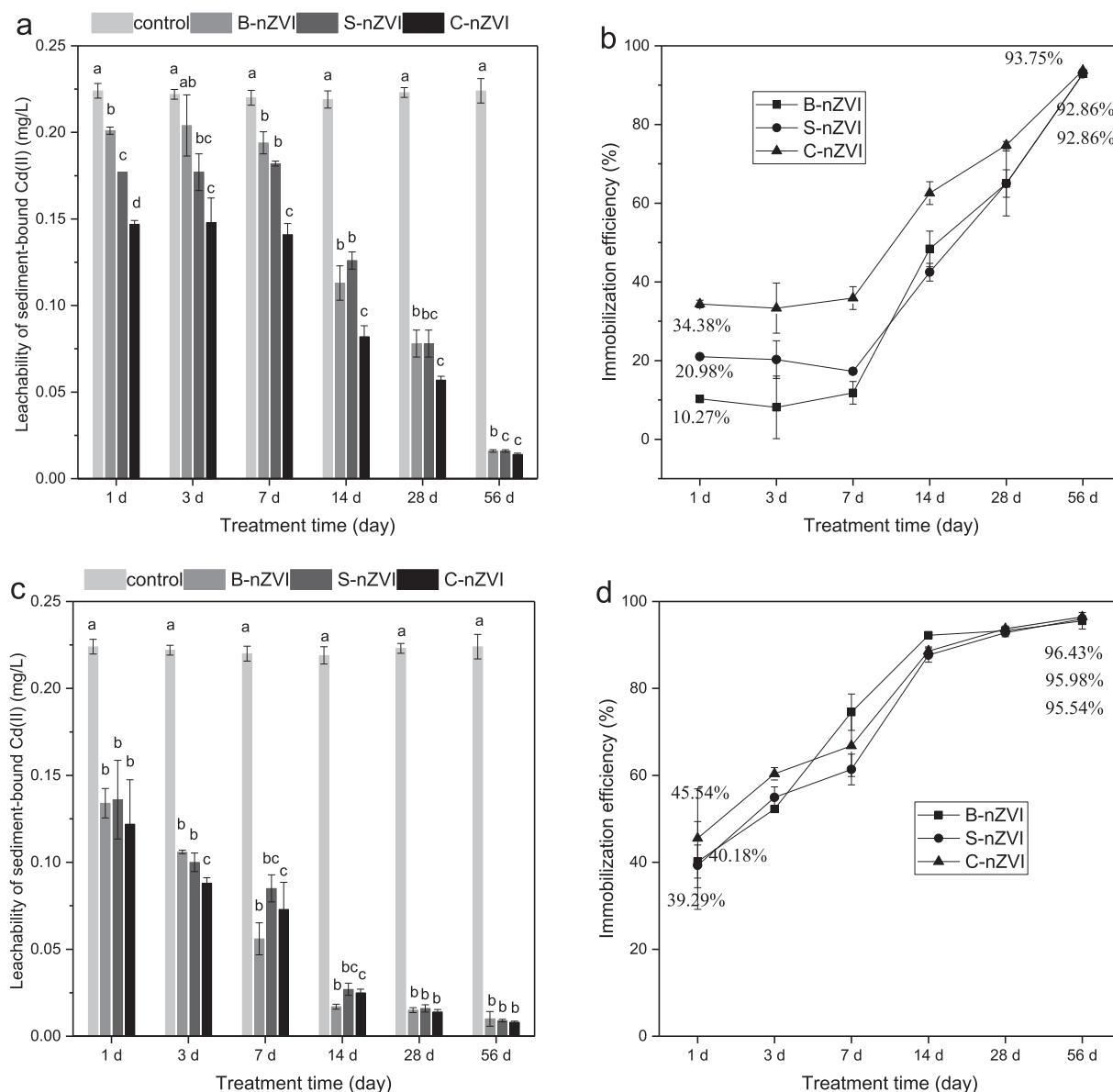


Fig. 2. The TCLP-based leachability of Cd(II) and immobilization efficiency at various treatment time when the sediment samples were treated by B-nZVI, S-nZVI and C-nZVI suspensions: (a and b) case 1 (0.5 g/L); and (c and d) case 2 (1.0 g/L). Bars with the same letters are not significantly different ($P < .05$).

Cd(II) was mainly bound to AS and RE (approximately 43.5% and 37.8%) while the OX and RS fractions occupied 12.5% and 6.2%, respectively. Fig. 4 reveals the ineffective immobilization of Cd(II) in the DI water treated sediment samples. In comparison, when the sediment samples were treated with nanoparticles, the Cd(II) speciation was altered to a different extent (Fig. 5): the AS fraction decreased with time while the RS fraction increased; the OX fraction decreased slightly while the RE fraction fluctuated within range of 25–40%. This phenomenon might result from the change of the redox potential that facilitates the transformation from the OX fraction to the AS fraction while not working for the RE fraction (Wen et al., 2016). At the same time, the adsorption or surface complex formation on the formed iron oxyhydroxide minerals could account for the decrease of the AS fraction (Zhang et al., 2014). The formation of FeOOH and Cd(II) complexation with FeOOH could be described by the following equations (Calderon and Fullana, 2015; Jr et al., 1996; Zhang et al., 2014):



Randall et al. (1999) reported that the bonding mechanism of the Cd(II) complexation with FeOOH was within the inner sphere of adsorption, which is quite stable. Therefore, the formed FeOCd⁺ or FeOCdOH could be deemed as the least available form, i.e., the residual fraction.

Additionally, it was evident that the AS fraction was more easily transformed to the RS fraction than the RE and OX fractions. The RE

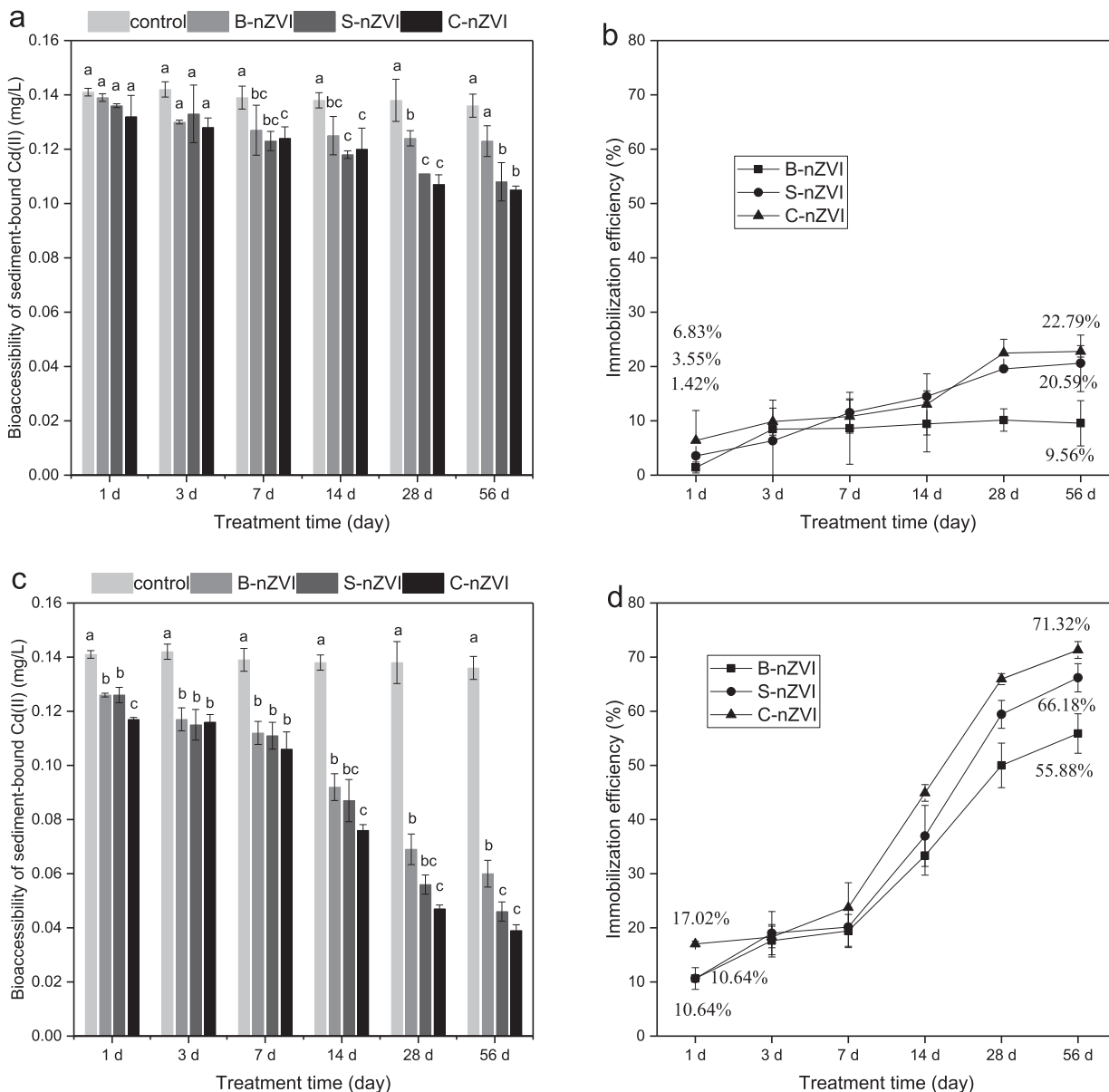


Fig. 3. The PBET-based bioaccessibility of Cd(II) and immobilization efficiency at various treatment time when the sediment samples were treated by B-nZVI, S-nZVI and C-nZVI suspensions: (a and b) case 1 (0.5 g/L); and (c and d) case 2 (1.0 g/L). Bars with the same letters are not significantly different ($P < .05$).

fraction was usually bound to hydrous oxides and amorphous iron/manganese oxides, and the OX fraction was combined with organics. These combinations were relatively stable, but the bound-metals might be liberated when the heterocomplex experienced oxidative or reductive effects (Wan et al., 2016; Wen et al., 2016). Generally, the organically bound-Cd(II) (RE fraction) could be transformed to the AS fraction in the presence of oxidizable zero-valent iron, while it was not. It is possible that the changes of the external conditions, such as the pH or enclosed space, caused the fluctuations of the RE fraction of Cd(II) (Fuentes et al., 2008; Gil-Díaz et al., 2014b). It was found that the stabilized nZVI (especially the C-nZVI) was more effective for immobilizing the AS fraction of Cd(II) than B-nZVI when adding equal doses for 56 days. This result is consistent with the results obtained from the TCLP and PBET tests. These changes in Cd(II) speciation indicate that stabilized nZVI might be quite durable and that using it is a possible solution to alleviate the mobility and bioavailability of Cd(II).

3.3. Nanoparticle transport in porous media

In the interest of fully confirming the practicality of stabilized nZVI, we need to examine its transport in a simulated groundwater environment. Fig. 6 presents the schematic drawing of the column experiments. The measured parameters and representative breakthrough curves (BTCs) for the column experiments are shown in Table 2 and Fig. 7. The data shows that B-nZVI exhibited a significant retention (elution levels (average C/C_0) < 20%) in both media. In contrast, the stabilized nZVI exhibited a higher mobility. For instance, the elution level in quartz sand was 68% for CMC- and 52% for starch-nZVI (Fig. 7a). C-nZVI was found to display a higher mobility than S-nZVI (Fig. 7b); this divergence in transport behaviour was likely linked to differences in the chemistries of the polysaccharides on the surface of the nZVI. The chemical composition of the polysaccharide functionalized the surface of nZVI and influenced the nZVI affinity of the sediment surface (Saleh et al.,

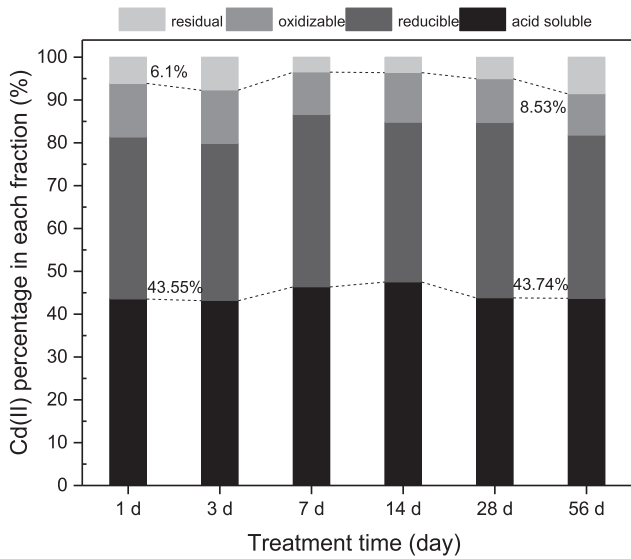


Fig. 4. The Cd(II) percentage in each fraction in the sediment incubated with deionized water from 0 to 56 days (in the control).

2008; Torkzaban et al., 2010). In addition, a 40% elution level for CMC- and a 20% level for starch-nZVI in sediment-supplemented quartz sand were observed (Fig. 7b). More nanoparticle retention occurred in sediment-supplemented quartz sand compared with

that in quartz sand (Fig. 7a). This phenomenon was consistent with the results of previous studies (Basnet et al., 2015; Kim et al., 2012; Pelley and Tufenkji, 2008; Quevedo and Tufenkji, 2012), in which the enhanced nanoparticle retention was attributed to the geochemical heterogeneity and potential for the physical straining of the sediment-supplemented quartz sand (e.g., presence of sediment). Additionally, the velocity U (Table 2) under equivalent injection pressures in different porous media was significantly different, indicating that the sediment produced a blocking effect during nanoparticle migration (Basnet et al., 2015).

The maximum travel distance L_{max} was estimated based on the classic filtration theory (Eq. 5(8)), and was directly related to the migration velocity U (He et al., 2009; Tufenkji and Elimelech, 2004; Xie et al., 2015). For a given velocity, L_{max} was calculated and is shown in Table S3. There were significant decreases of L_{max} when applying to sediment-supplemented quartz sand (Fig. 8). This result suggests that the transport distance of nanoparticles was rather confined under this groundwater flow condition (only ~18 cm for B-nZVI), while polysaccharide stabilizers such as starch or CMC could extend the travel distance; however, inherent site physical and chemical heterogeneities remained as challenges for nanoparticle transport.

3.4. Potential mechanism and challenges of stabilized nZVI treatment

Because of the nearly identical standard potentials of cadmium and zero-valent iron, the mechanism of Cd(II) immobilization via stabilized nZVI is likely adsorption or surface complex formation instead of direct reduction. Note that stabilized nZVI would not

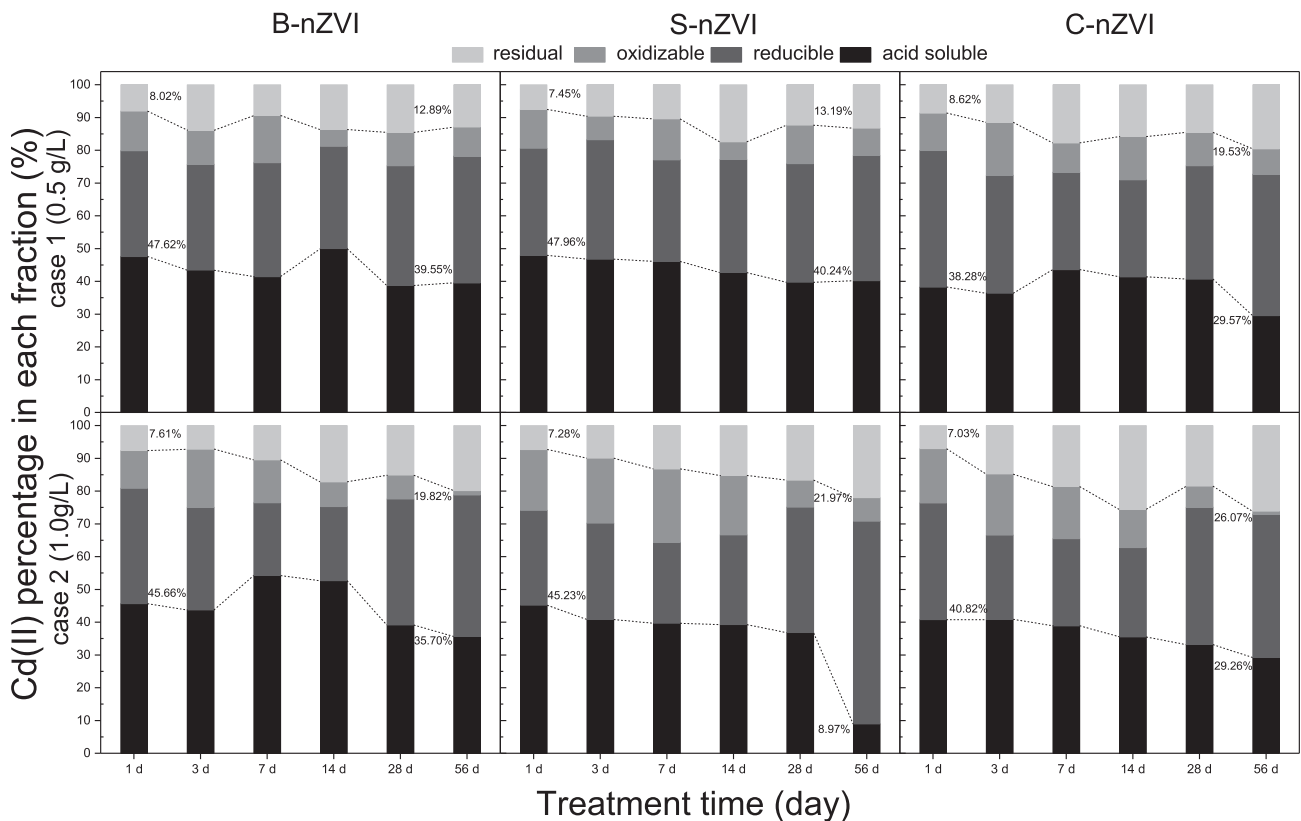


Fig. 5. Changes of the Cd(II) speciation at various treatment time when the sediment samples were treated by B-nZVI, S-nZVI and C-nZVI in case 1 (0.5 g/L) and case 2 (1.0 g/L).

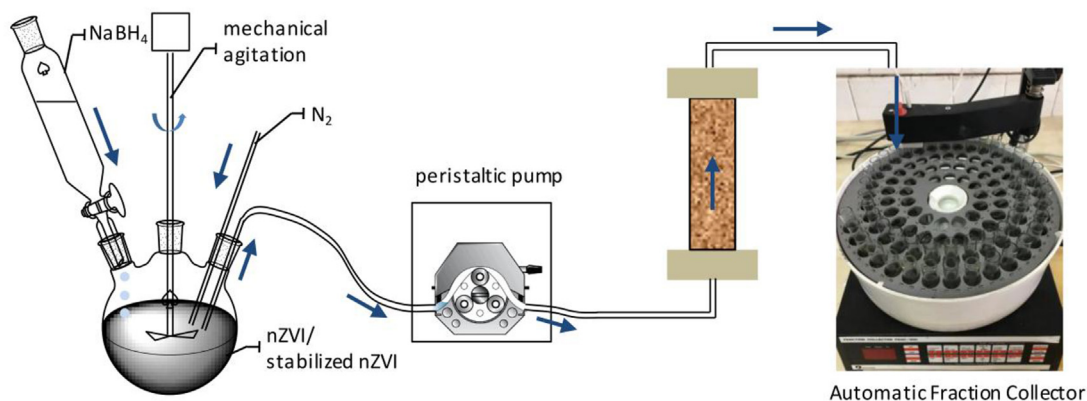


Fig. 6. Schematic drawing of the column experiments.

Table 2

Parameters of quartz sand column and sediment-supplemented quartz sand column for the B-nZVI, S-nZVI and C-nZVI transport experiments.

Parameter	Quartz sand column	Sediment-supplemented quartz sand column
Flow rate (mL/min), Q	0.556	0.111
Pore volume (mL), PV	11.273	10.975
Porosity, θ	0.467	0.455
Column height (cm), L	15	15
Column inner diameter (cm), D_i	1.6	1.6
Packed height in the column (cm)	12	12
Velocity (cm/s), U	0.0046	0.0009
Average particle size of media (μm)	302.4	292

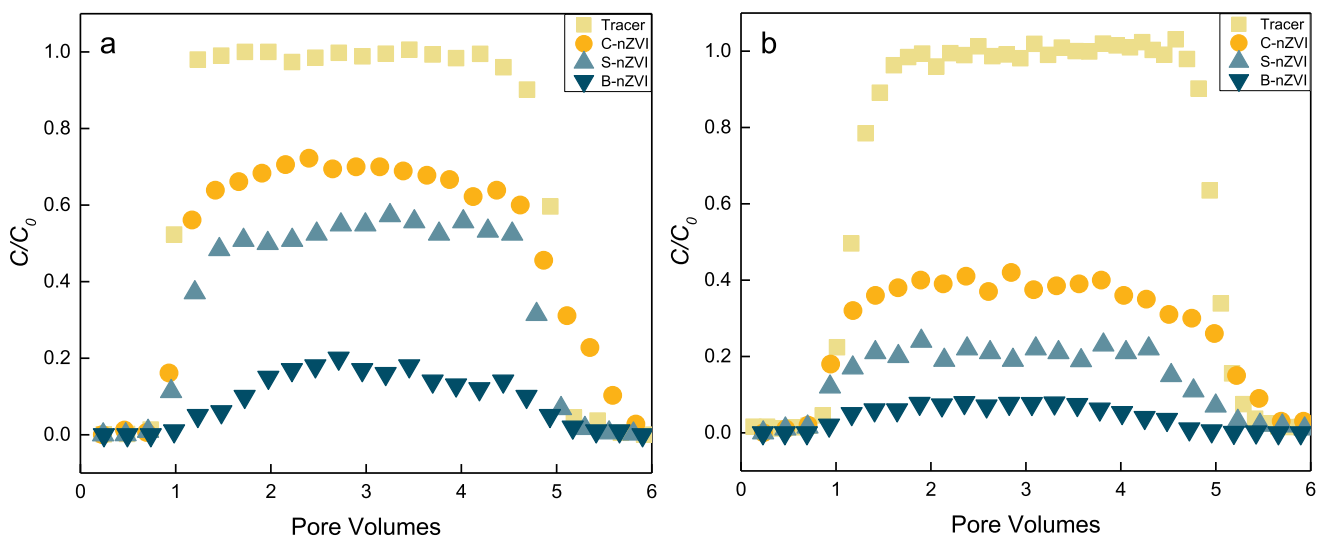


Fig. 7. Measured breakthrough curves for B-nZVI, S-nZVI and C-nZVI in (a) quartz sand and (b) sediment-supplemented quartz sand. The concentration of the tested nanoparticle suspensions is 1.0 g/L. The breakthrough behaviour of an inert tracer (10 mM KNO_3) is also presented.

keep the pristine nZVI throughout the whole sediment remediation even though stabilizers were present. The emulsified nZVI could be mostly transformed to magnetite, lepidocrocite and goethite within a few months. Su et al. (2013) confirmed this conclusion and attributed this to the ageing effect of stabilized nZVI. Thus, for longer reaction times, the effects of stabilizers on nZVI might be to prolong reactivity and maintain the physical and chemical integrities (He and Zhao, 2005). Due to the presence of CMC or starch, nZVI had adequate time to reach the contaminated subsurface zones and capture the soluble Cd(II). With ageing, the

polysaccharide coating might be removed from nZVI and degraded or modified by species already present in sediment, resulting in aqueous corrosion of the nZVI and the continuous formation of iron oxyhydroxide minerals (Eqs. (3)–(5)). Subsequently, the formed iron oxyhydroxide minerals would produce continuous adsorption of the TCLP leachability/PBET bioaccessibility of Cd(II) and the AS fraction of Cd(II) (Eqs. (6)–(7)). Finally, the formed FeOCD^+ or FeOCDOH was deemed as the least available form that could resist the acid extraction. This conclusion was confirmed by the TCLP tests (3.2.1): immobilization efficiency of the TCLP leachability of Cd(II)

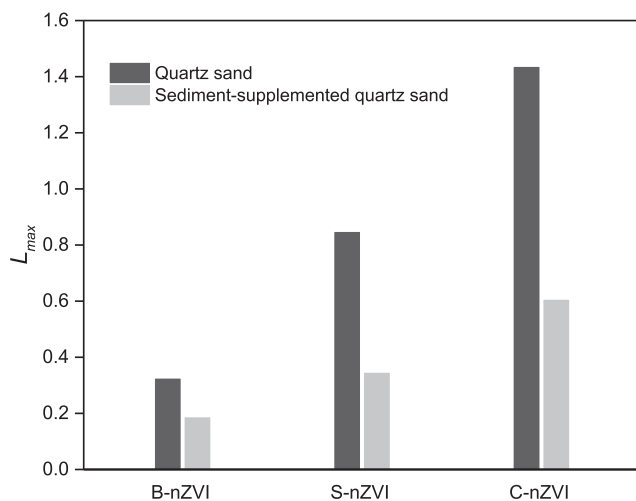


Fig. 8. The maximum transport distance (L_{max}) of B-nZVI, S-nZVI and C-nZVI in quartz sand and sediment-supplemented quartz sand.

was at a comparatively low level within 14 days and increased significantly after 14 days. On the other hand, H^+ appeared during the formation of $FeOOH$ (Eq. (5)). The surface hydroxyl groups in the stabilizers might be protonated to OH_2^+ , resulting in more and stronger sorption sites for the heavy metals (An and Zhao, 2012). This might be another positive effect of the stabilizers.

The stability of the metals immobilized by nZVI was confirmed by several authors. Gil-Díaz et al. (2014a) reported that Pb or Zn immobilization was stable after simulating 2 years of typical annual rainfall in Spain. Chen et al. (2016) found that nZVI/AC had a relatively long-term stabilization effect on multi-metal contaminated sediment. Even so, the long-term stability of the immobilized Cd(II) is still important to consider. Part of the inert Cd(II) is likely to be remobilized and transformed into a toxic fraction again due to long-term processes or changes of the environmental conditions (Calderon and Fullana, 2015). What is more, the polysaccharide coating applied to protect the metallic iron core is still vulnerable to changing environmental conditions. The inherent physical and chemical heterogeneities of the aquifer material in groundwater environments remain further major challenges for the development of the functional relationships between nanoparticle transport potential and sediment properties. Thus, further studies are needed to reveal the potential effects of environmental conditions on the effectiveness of C-nZVI (or S-nZVI) applications for a wider range of environmental media.

4. Conclusions

Results from the batch and column experiments verified the effectiveness of the stabilized nZVI for Cd(II) immobilization in sediment. Experimental data showed that the stabilized nZVI could effectively decrease the TCLP leachability and the PBET bioaccessibility of Cd(II). At the same time, the AS fraction of Cd(II) was partially transformed into a residual fraction. Adsorption or surface complex formation on the formed iron oxyhydroxide layer is the most likely a mechanism of Cd(II) immobilization. Additionally, compared to B-nZVI and S-nZVI, C-nZVI had a better immobilization effect, and the increase of the nanoparticle dose (such as 10 mg/g-sediment as Fe^0) could improve the immobilization efficiency of Cd(II). Column experiments indicated that stabilized nZVI (especially the C-nZVI) exhibited an enhanced transport and left less retention in porous media, but inherent sites with physical and

chemical heterogeneities still posed challenges for nanoparticle transport. What is more, the long-term stability of the immobilized Cd(II) needs to be further investigated due to the long-term processes or changes of the environmental conditions. Overall, for the Xiang River, which is currently found to be Cd(II) rich, using stabilized nZVI-coated by polysaccharide is an effective pathway to alleviate the hazards likely posed to the environment, especially in consideration of the high valued utilization of sediment in land applications.

Acknowledgements

This work was supported by the Program for the National Natural Science Foundation of China (51579098, 51378190, 51278176, 51408206, 51521006), the National Program for Support of Top-Notch Young Professionals of China (2014), Hunan Provincial Science and Technology Plan Project (No.2016RS3026), the Program for New Century Excellent Talents in University (NCET-13-0186) and the Program for Changjiang Scholars and Innovative Research Team in University (IRT-13R17).

Appendix A. Supplementary data

Supplementary data related to this article can be found at <https://doi.org/10.1016/j.jenvman.2018.01.001>.

References

- Ambika, S., Nambi, I.M., Senthilnathan, J., 2016. Low temperature synthesis of highly stable and reusable CMC- Fe^{2+} -nZVI catalyst for the elimination of organic pollutants. *Chem. Eng. J.* 289, 544–553.
- An, B., Zhao, D., 2012. Immobilization of As(III) in soil and groundwater using a new class of polysaccharide stabilized Fe-Mn oxide nanoparticles. *J. Hazard. Mater.* 211–212, 332–341.
- Arshadi, M., Soleymanzadeh, M., Salvacion, J.W.L., Salimivahid, F., 2014. Nanoscale Zero-Valent Iron (nZVI) supported on sineguas waste for Pb(II) removal from aqueous solution: kinetics, thermodynamic and mechanism. *J. Colloid Interface Sci.* 426, 241–251.
- Basnet, M., Tommaso, C.D., Ghoshal, S., Tufenkji, N., 2015. Reduced transport potential of a palladium-doped zero valent iron nanoparticle in a water saturated loamy sand. *Water Res.* 68, 354–363.
- Boparai, H.K., Joseph, M., O'Carroll, D.M., 2013. Cadmium (Cd^{2+}) removal by nano zerovalent iron: surface analysis, effects of solution chemistry and surface complexation modeling. *Environ. Sci. Pollut. Res.* 20, 6210–6221.
- Burton, G.A., 2002. Sediment quality criteria in use around the world. *Limnology* 3, 65–76.
- Calderon, B., Fullana, A., 2015. Heavy metal release due to aging effect during zero valent iron nanoparticles remediation. *Water Res.* 83, 1–9.
- Chen, P.J., Tan, S.W., Wu, W.L., 2012. Stabilization or oxidation of nanoscale zero-valent iron at environmentally relevant exposure changes bioavailability and toxicity in medaka fish. *Environ. Sci. Technol.* 46, 8431–8439.
- Chen, W.F., Zhang, J., Zhang, X., Wang, W., Li, Y., 2016. Investigation of heavy metal (Cu, Pb, Cd, and Cr) stabilization in river sediment by nano-zero-valent iron/activated carbon composite. *Environ. Sci. Pollut. Res.* 23, 1460–1470.
- Cheng, M., Zeng, G., Huang, D.L., Lai, C., Xu, P., Zhang, C., Liu, Y., 2016. Hydroxyl radicals based advanced oxidation processes (AOPs) for remediation of soils contaminated with organic compounds: a review. *Chem. Eng. J.* 284, 582–598.
- Chou, J.D., Wey, M.Y., Liang, H.H., Chang, S.H., 2009. Biototoxicity evaluation of fly ash and bottom ash from different municipal solid waste incinerators. *J. Hazard. Mater.* 168, 197–202.
- Fuentes, A., Llorens, M., Saez, J., Isabel, M.A., Ortuno, J.F., Meseguer, V.F., 2008. Comparative study of six different sludges by sequential speciation of heavy metals. *Bioresour. Technol.* 99, 517–525.
- Geebelen, W., Adriano, D.C., Lelie, D.V.D., Mench, M., Carleer, R., Clijsters, H., Vangronsveld, J., 2003. Selected bioavailability assays to test the efficacy of amendment-induced immobilization of lead in soils. *Plant Soil* 249, 217–228.
- Gil-Díaz, M., Ortiz, L.T., Costa, G., Alonso, J., Rodríguez-Membibre, M.L., Sánchez-Fortún, S., Pérez-Sanz, A., Martín, M., Lobo, M.C., 2014a. Immobilization and leaching of Pb and Zn in an acidic soil treated with zerovalent iron nanoparticles (nZVI): physicochemical and toxicological analysis of leachates. *Water Air Soil Pollut.* 225, 1–13.
- Gil-Díaz, M., Pérez-Sanz, A., Ángeles Vicente, M., Carmen Lobo, M., 2014b. Immobilisation of Pb and Zn in soils using stabilised zero-valent iron nanoparticles: effects on soil properties. *Clean Soil Air Water* 42, 1776–1784.
- Hakanson, L., 1980. An ecological risk index for aquatic pollution control—a sedimentological approach. *Water Res.* 14, 975–1001.

- He, F., Zhang, M., Qian, T., Zhao, D., 2009. Transport of carboxymethyl cellulose stabilized iron nanoparticles in porous media: column experiments and modeling. *J. Colloid Interface Sci.* 334, 96–102.
- He, F., Zhao, D., 2005. Preparation and characterization of a new class of starch-stabilized bimetallic nanoparticles for degradation of chlorinated hydrocarbons in water. *Environ. Sci. Technol.* 39, 3314–3320.
- He, F., Zhao, D., 2007. Manipulating the size and dispersibility of zerovalent iron nanoparticles by use of carboxymethyl cellulose stabilizers. *Environ. Sci. Technol.* 41, 6216–6221.
- He, F., Zhao, D., Liu, J., Roberts, C.B., 2007. Stabilization of Fe–Pd nanoparticles with sodium carboxymethyl cellulose for enhanced transport and dechlorination of trichloroethylene in soil and groundwater. *Ind. Eng. Chem. Res.* 46, 29–34.
- Huang, D.L., Chen, G.M., Zeng, G., Xu, P., Yan, M., Lai, C., Zhang, C., Li, N.J., Cheng, M., He, X.X., He, Y., 2015. Synthesis and application of modified zero-valent iron nanoparticles for removal of hexavalent chromium from wastewater. *Water Air Soil Pollut.* 226, 1–14.
- Huang, D.L., Xue, W., Zeng, G., Wan, J., Chen, G., Huang, C., Zhang, C., Cheng, M., Xu, P., 2016. Immobilization of Cd in river sediments by sodium alginate modified nanoscale zero-valent iron: impact on enzyme activities and microbial community diversity. *Water Res.* 106, 15–25.
- Huang, D.L., Zeng, G., Feng, C.L., Hu, S., Jiang, X.Y., Tang, L., Su, F.F., Zhang, Y., Zeng, W., Liu, H.L., 2008. Degradation of lead-contaminated lignocellulosic waste by *Phanerochaete chrysosporium* and the reduction of lead toxicity. *Environ. Sci. Technol.* 42, 4946–4951.
- Jaisi, D.P., Elimelech, M., 2009. Single-walled carbon nanotubes exhibit limited transport in soil columns. *Environ. Sci. Technol.* 43, 9161–9166.
- Jiang, J., Wang, J., Xu, X., Wang, W., Zhou, D., Zhang, Y., 2004. Heavy metal stabilization in municipal solid waste incineration flyash using heavy metal chelating agents. *J. Hazard. Mater.* 113, 141–146.
- Jr, R., Bp, H., Ar, F., 1996. Molecular statics calculations for iron oxide and oxyhydroxide minerals: toward a flexible model of the reactive mineral-water interface. *Geochem. Cosmochim. Acta* 60, 1553–1562.
- Kambhu, A., Comfort, S., Chokeyaroenrat, C., Sakulthaew, C., 2012. Developing slow-release persulfate candles to treat BTEX contaminated groundwater. *Chemosphere* 89, 656–664.
- Kim, H.J., Phenrat, T., Tilton, R.D., Lowry, G.V., 2012. Effect of kaolinite, silica fines and pH on transport of polymer-modified zero valent iron nano-particles in heterogeneous porous media. *J. Colloid Interface Sci.* 370, 1–10.
- Kim, S.A., Kamala-Kannan, S., Lee, K.J., Park, Y.J., Shea, P.J., Lee, W.H., Kim, H.M., Oh, B.T., 2013. Removal of Pb(II) from aqueous solution by a zeolite–nanoscale zero-valent iron composite. *Chem. Eng. J.* 217, 54–60.
- Lee, S.H., Park, H., Koo, N., Hyun, S., Hwang, A., 2011. Evaluation of the effectiveness of various amendments on trace metals stabilization by chemical and biological methods. *J. Hazard. Mater.* 188, 44–51.
- Lian, X., Liu, L., Guo, J., Li, L., Wu, C., 2013. Screening of seeds prepared from retrograded potato starch to increase retrogradation rate of maize starch. *Int. J. Biol. Macromol.* 60, 181–185.
- Lin, Y.H., Tseng, H.H., Wey, M.Y., Lin, M.D., 2010. Characteristics of two types of stabilized nano zero-valent iron and transport in porous media. *Sci. Total Environ.* 408, 2260–2267.
- Ling, L., Pan, B., Zhang, W.X., 2015. Removal of selenium from water with nanoscale zero-valent iron: mechanisms of intraparticle reduction of Se(IV). *Water Res.* 71, 274–281.
- Liu, L., Chen, H., Cai, P., Liang, W., Huang, Q., 2009. Immobilization and phytotoxicity of Cd in contaminated soil amended with chicken manure compost. *J. Hazard. Mater.* 163, 563–567.
- Liu, R., Zhao, D., 2007. Reducing leachability and bioaccessibility of lead in soils using a new class of stabilized iron phosphate nanoparticles. *Water Res.* 41, 2491–2502.
- Maity, D., Agrawal, D.C., 2007. Synthesis of iron oxide nanoparticles under oxidizing environment and their stabilization in aqueous and non-aqueous media. *J. Magn. Magn. Mater.* 308, 46–55.
- Moral, R., Cortés, A., Gomez, I., Mataix-Beneyto, J., 2002. Assessing changes in Cd phytoavailability to tomato in amended calcareous soils. *Bioresour. Technol.* 85, 63–68.
- Pelley, A.J., Tufenkji, N., 2008. Effect of particle size and natural organic matter on the migration of nano- and microscale latex particles in saturated porous media. *J. Colloid Interface Sci.* 321, 74–83.
- Quevedo, I.R., Tufenkji, N., 2012. Mobility of functionalized quantum dots and a model polystyrene nanoparticle in saturated quartz sand and loamy sand. *Environ. Sci. Technol.* 46, 4449–4457.
- Randall, S.R., Sherman, D.M., Ragnarsdottir, K.V., Collins, C.R., 1999. The mechanism of cadmium surface complexation on iron oxyhydroxide minerals. *Geochem. Cosmochim. Acta* 63, 2971–2987.
- Ruby, M.V., Davis, A., Schoof, R., Eberle, S., Sellstone, C.M., 1996. Estimation of lead and arsenic bioavailability using a physiologically based extraction test. *Environ. Sci. Technol.* 30, 422–430.
- Saleh, N., Kim, H.J., Phenrat, T., Matyjaszewski, K., Tilton, R.D., Lowry, G.V., 2008. Ionic strength and composition affect the mobility of surface-modified Fe⁰ nanoparticles in water-saturated sand columns. *Environ. Sci. Technol.* 42, 3349–3355.
- Sharp, A., Turner, A., 2013. Concentrations and bioaccessibilities of trace elements in barbecue charcoals. *J. Hazard. Mater.* 262, 620–626.
- Shi, L.N., Zhang, X., Chen, Z.L., 2011. Removal of chromium (VI) from wastewater using bentonite-supported nanoscale zero-valent iron. *Water Res.* 45, 886–892.
- Su, H., Fang, Z., Tsang, P.E., Fang, J., Zhao, D., 2016. Stabilisation of nanoscale zero-valent iron with biochar for enhanced transport and *in-situ* remediation of hexavalent chromium in soil. *Environ. Pollut.* 214, 94–100.
- Su, C., Puls, R.W., Krug, T.A., Watling, M.T., O'Hara, S.K., Quinn, J.W., Ruiz, N.E., 2013. Travel distance and transformation of injected emulsified zerovalent iron nanoparticles in the subsurface during two and half years. *Water Res.* 47, 4095–4106.
- Torkzaban, S., Kim, Y., Mulvihill, M., Wan, J., Tokunaga, T.K., 2010. Transport and deposition of functionalized CdTe nanoparticles in saturated porous media. *J. Contam. Hydrol.* 118, 208–217.
- Tufenkji, N., Elimelech, M., 2004. Correlation equation for predicting single-collector efficiency in physicochemical filtration in saturated porous media. *Environ. Sci. Technol.* 39, 529–536.
- Wan, J., Zhang, C., Zeng, G., Huang, D.L., Hu, L., Huang, C., Wu, H., Wang, L., 2016. Synthesis and evaluation of a new class of stabilized nano-chlorapatite for Pb immobilization in sediment. *J. Hazard. Mater.* 320, 278–288.
- Wang, F.H., Zhao, B., Zhang, F., Gao, J., Hao, H.T., Zhang, S., 2015. A novel heavy metal chelating agent sixthio guanidine acid for *in situ* remediation of soils contaminated with multielements: its synthesis, solidification, biodegradability, and leachability. *J. Soils Sediments* 16, 371–381.
- Wang, L., Yuan, X., Zhong, H., Wang, H., Wu, Z., Chen, X., Zeng, G., 2014. Release behavior of heavy metals during treatment of dredged sediment by microwave-assisted hydrogen peroxide oxidation. *Chem. Eng. J.* 258, 334–340.
- Wen, J., Yi, Y., Zeng, G., 2016. Effects of modified zeolite on the removal and stabilization of heavy metals in contaminated lake sediment using BCR sequential extraction. *J. Environ. Manag.* 178, 63–69.
- Weng, X., Lin, S., Zhong, Y., Chen, Z., 2013. Chitosan stabilized bimetallic Fe/Ni nanoparticles used to remove mixed contaminants-amoxicillin and Cd (II) from aqueous solutions. *Chem. Eng. J.* 229, 27–34.
- Wu, S., Shen, Z., Yang, C., Zhou, Y., Li, X., Zeng, G., Ai, S., He, H., 2017. Effects of C/N ratio and bulking agent on speciation of Zn and Cu and enzymatic activity during pig manure composting. *Int. Biodeter. Biodegr.* 119, 429–436.
- Xie, W., Liang, Q., Qian, T., Zhao, D., 2015. Immobilization of selenite in soil and groundwater using stabilized Fe–Mn binary oxide nanoparticles. *Water Res.* 70, 485–494.
- Xu, P., Zeng, G., Huang, D.L., Feng, C.L., Hu, S., Zhao, M.H., Lai, C., Wei, Z., Huang, C., Xie, G.X., 2012. Use of iron oxide nanomaterials in wastewater treatment: a review. *Sci. Total Environ.* 424, 1–10.
- Zhang, Y., Li, Y., Dai, C., Zhou, X., Zhang, W., 2014. Sequestration of Cd(II) with nanoscale zero-valent iron (nZVI): characterization and test in a two-stage system. *Chem. Eng. J.* 244, 218–226.